

## THE EFFECT OF KENAF FIBRE LOADING ON CURING CHARACTERISTICS AND MECHANICAL PROPERTIES OF WASTE TYRE DUST/ KENAF FIBRE HYBRID FILLER FILLED NATURAL RUBBER COMPOUNDS

Hanafi Ismail,<sup>a,\*</sup> Nurul Farhana Omar,<sup>a</sup> and Nadras Othman<sup>a</sup>

Waste tyre dust (WTD)/kenaf fibre (Ke) hybrid filler filled natural rubber (NR) compounds having constant 30 phr loading were prepared with increasing partial replacement of WTD by kenaf fibre at 0, 10, 15, 20, and 30 phr. Curing characteristics, mechanical properties, rubber-fibre interaction, and morphology of the NR compounds were studied after the compounds were obtained. The curing characteristics such as  $t_2$  and  $t_{90}$  increased with increment of kenaf fibre loading. For  $M_{HR}$ , the increasing partial replacement of WTD by kenaf fibre showed increasing  $M_{HR}$  value. For tensile properties, the value of tensile strength and elongation at break value decreased with increasing kenaf fibre loading. The values of  $M100$  and  $M300$  increased but then decreased after the addition of 15 phr of kenaf fibre loading. Besides, fatigue life value also showed a decreasing trend with increasing kenaf fibre loading. For rubber-fibre interaction, the values of  $Q_f/Q_g$  showed a small increment with increasing kenaf fibre loading. The SEM micrographs obtained for fractured surface of WTD/kenaf fibre hybrid filled NR compounds supported the results for the mechanical properties.

*Keywords:* Curing characteristics; Tensile properties; Natural rubber; Waste tyre dust; Kenaf fibre

*Contact information:* a: School of Materials and Mineral Resources Engineering, Engineering Campus, Seri Ampangan, Universiti Sains Malaysia, Nibong Tebal, Seberang Perai Selatan, Penang, Malaysia;

\* Corresponding author: hanafi@eng.usm.my

### INTRODUCTION

Natural fibres have favorable attributes such as low price, low density, and also good affinity for polar polymer matrices (Huda et al. 2004). Among natural fibres produced today, there are certain fibres frequently used that come from a class of plants known for their fibers, e.g. jute, flax, ramie, bamboo, abaca, sisal, and kenaf (Suzuki et al. 2004). Kenaf is one of the most well known and utilized fibres today. Kenaf, which is also known scientifically as *Hibiscus cannabinus* L (Bada et al. 2010), is one of the natural fibres planted globally. Like the other mentioned fibres, kenaf is known for its role in applications involving reinforcement. Kenaf plants are comprised of multiple useful components. Kenaf's stem and bark have high quality fibres that are suitable for various applications. There are several products that can be made by using kenaf, e.g. paper-based products, clothes, construction materials, car accessories, biofuels, animal feed (Hamid 2008), and chemical absorbents (Bada et al. 2010). Besides all the mentioned applications, kenaf can also be applied in reinforcement applications. In

general the use of natural fibres like kenaf can provide better alternatives towards achievement of environmental sustainability.

Besides using kenaf, another method to save the environment is by recycling or reutilization of waste products. Tyres create a serious waste problem for the environment and a burden for landfill operations due to their ever-increasing production. Considerable efforts have been made in reducing the disposal of waste tyre. The Scrap Tyre Management Council estimates that of the 266 million scrap tyres generated in the United States, approximately 24.5 million were recycled in 1996 for purposes such as ground rubber in products and asphalt highways, stamped products, and agricultural and miscellaneous uses. An additional 10 million were beneficially used in civil engineering projects (Park et al. 2003). Currently, the incorporation of shredded waste tyres or waste tyre crumb in cement or concrete have become popular, as the addition of waste tyre into cement can improve the performance of the cement in term of toughness and ductility (Yilmaz et al. 2009; Segre et al. 2002; Benazzouk et al. 2008) in construction applications. Besides, the shredded scrap tyre or waste tyre dust has also been studied with respect to leachate (Park et al. 2003), and as filler for composites or compounds (Awang et al. 2009). Therefore, as kenaf fibre is able to act as reinforcement, it was chosen to be paired with WTD as hybrid filler for natural rubber (NR) compound in this work. The objective of the pairing is to study the mechanical properties, which involve tensile properties and fatigue life as well as curing characteristics, swelling behaviour, and morphology of WTD/kenaf fibre hybrid filler filled NR compounds.

## EXPERIMENTAL

### Materials

Table 1 shows the formulation used in this study. The natural rubber (SMR L) was purchased from Kumpulan Guthrie Sdn. Bhd., Seremban, Malaysia. The waste tyre dust (WTD) was obtained from Watas Holding (M) Sdn. Bhd., Penang, Malaysia.

**Table 1.** Formulation of WTD/Kenaf Fibre Hybrid Filler Filled Natural Rubber Compounds

Ingredients/compounds	WTD30/ Ke 0	WTD20/ Ke 10	WTD15/ Ke 15	WTD10/ Ke 20	WTD0/ Ke 30
Natural rubber (SMR L)	100	100	100	100	100
Waste tyre dust (WTD)	30	20	15	10	0
Kenaf fibre (Ke)	0	10	15	20	30
Zinc oxide (ZnO)	5	5	5	5	5
Stearic acid	2	2	2	2	2
Sulphur (S)	2.5	2.5	2.5	2.5	2.5
N-cyclohexyl-2-benzothiazole sulfonamide (CBS)	0.6	0.6	0.6	0.6	0.6
2, 2'-Methylene-bis (4-methyl-6-tert-butylphenol) (BKF)	2	2	2	2	2

An Endecotts sieve was used to obtain WTD particle size of 150 to 250  $\mu\text{m}$ . Kenaf fibre (Ke) was obtained from Forest Research Institute of Malaysia (FRIM). The fibres were soaked and cleaned with tap water and cut to the average length and diameter of 7700  $\mu\text{m}$  and 30.5  $\mu\text{m}$ , respectively. Other compounding ingredients such as zinc oxide, stearic acid, sulphur, N-cyclohexyl-2-benzothiazole sulfonamide (CBS), and 2,2'-Methylene-bis (4-methyl-6-tert-butylphenol) (BKF) were all purchased from Bayer (M) Ltd.

### Preparation of Rubber Compound

Mixing was carried out using a conventional laboratory two roll mill size ( $160 \times 320 \text{ mm}^2$ ) according to ASTM designation D3184-80. Nip gap, mill roll speed ratio, time of mixing, and the sequence of addition of the ingredients were kept the same for all the composites. The sheeted rubber compound was conditioned at a temperature of  $23 \pm 2^\circ\text{C}$  for 24 h in a closed container before cure assessment, using a Monsanto moving die rheometer (MDR 2000). The respective scorch time ( $t_2$ ) and cure time ( $t_{90}$ ) were obtained from MDR 2000 at  $150^\circ\text{C}$ . The maximum torque was also determined from the rheograph. The rubber compounds were compression moulded at  $150^\circ\text{C}$  according to their respective  $t_{90}$  values into 2 types of rectangular sheets: one was with the size of 229 mm  $\times$  76 mm  $\times$  1.5 mm with beaded edges (fatigue test), and another one was flatter sheet with 2mm thickness (tensile test).

### Determination of Tensile Properties

Dumbbell specimens were cut out from compression moulded sheets. The tensile test was conducted following ASTM D412 using a universal tensile testing machine Instron 3366 at room temperature ( $25 \pm 2^\circ\text{C}$ ) and with crosshead speed of 500 mm/min. Tensile modulus at 100% (M100) and 300% elongation (M300), tensile strength and elongation at break ( $E_b$ ) were recorded.

### Determination of Fatigue Life

The vulcanised NR was cut into individual dumbbell samples using a BS type E dumbbell cutter. Fatigue test of the NR compounds was then carried out on a Monsanto Fatigue-to-Failure Tester (FTFT). Six specimens were used for each test. The samples were subjected to repeated cyclic strain at  $100 \text{ rev min}^{-1}$  and the extension ratio of  $1.61 \pm 0.04$ . The number of cycles was recorded automatically. The fatigue life was calculated based on the Japanese Industrial Standard (JIS) average, which was determined from the four highest values recorded using the Equation (1):

$$\text{JIS average} = 0.5A + 0.3B + 0.1(C + D) \quad (1)$$

where A is the highest value followed by B, C, and D.

### Measurement of Rubber-Filler Interaction

Cured samples with the dimension 30 mm  $\times$  5 mm  $\times$  2 mm were immersed in toluene and kept in dark environment until equilibrium swelling was achieved, which normally took 48 h at  $25^\circ\text{C}$ . The samples were dried in the oven at  $60^\circ\text{C}$  until the constant

weights were obtained. The Lorenz and Park equation (Lorenz et al. 1961) was applied to study the rubber-filler interaction according to Equation (2),

$$Q_f/Q_g = ae^{-z} + b \quad (2)$$

where the subscripts f and g refer to filled and gum vulcanizates respectively;  $z$  is the ratio by weight of the filler to the rubber hydrocarbon in the vulcanizates; and  $a$  and  $b$  are constants. The higher the  $Q_f/Q_g$  values are, the lower will be the extent of interaction between the filler and the matrix. In this study, we determined the weight of toluene uptake per gram of rubber hydrocarbon ( $Q$ ) as Equation (3),

$$Q = (W_s - W_d)/(W_i \times 100/\text{Formula weight}) \quad (3)$$

where  $W_s$  is the swollen weight,  $W_d$  is the dried weight, and  $W_i$  is the original weight.

### Morphological Study

Scanning electron microscopy (SEM) model Zeiss SUPRA 35VP FESEM was used to characterise the WTD and fractured surface of WTD/CB hybrid filler filled natural rubber compounds. All the surfaces were examined by SEM after first sputter coating with gold to avoid electrostatic charging and poor resolution.

### Fourier Transform Infra Red (FTIR) Analysis

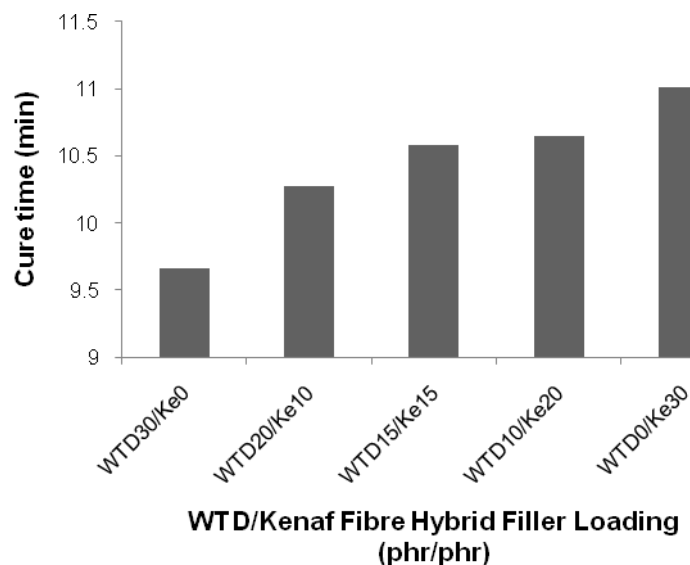
The chemical bonds in the WTD and kenaf fibre were analysed using a Perkin-Elmer Spectrum One FT-IR spectrometer. A sample of the WTD was prepared by milling it with KBr and compressed for testing while sample of kenaf fibre was tested in attenuated total reflection (FTIR-ATR) mode. The selected spectrum resolution was  $4 \text{ cm}^{-1}$  and the scanning range for WTD and kenaf fibre was ranged from  $400$  to  $4000 \text{ cm}^{-1}$ .

## RESULTS AND DISCUSSION

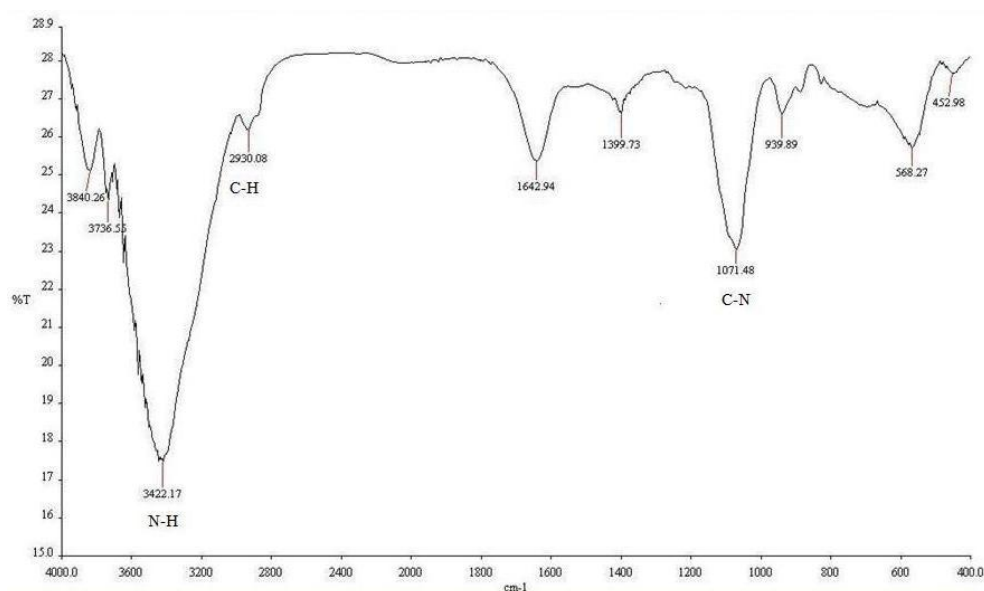
### Cure Time

Figure 1 shows the effect of WTD/kenaf fibre hybrid filler loading on cure time of natural rubber compounds. The natural rubber compounds prepared in this work were filled with 30 phr of WTD/kenaf fibre hybrid. This figure shows an increasing trend of cure time with the increment of kenaf fibre loading. The NR compounds with the highest amount of WTD exhibited the shortest cure time value. This effect is attributed to the presence of crosslinked precursors and unreacted curative in the WTD. As shown in Fig. 2, there were absorption bands or peaks due to N-H, C-N, and  $-\text{CH}_2$ . These groups are believed to exist in the unreacted accelerator within WTD. A non-hydrogen bonded N-H stretching symmetric vibration can be seen at  $3422 \text{ cm}^{-1}$ . Aliphatic C-N stretching is indicated by an adsorption band appearing at  $1071 \text{ cm}^{-1}$ , while methylene asymmetric C-H stretching is indicated by a band at  $2930 \text{ cm}^{-1}$  (Stuart 2004). These bonds are usually present in accelerator like N-Cyelohexy1-2-benzothiazole sulfonamide (CBS) with the chemical structure shown in Fig. 3. CBS posses sulphur element and is called sulphur

donor. In vulcanization process, CBS generates active sulphur fragments. Hence, these active sulphur fragments react with present rubber molecules and induce curing (Tampere University of Technology 2011). Therefore, higher amount of WTD promotes higher curing. The short value of cure time for the natural rubber compound filled with 30 phr of WTD indicates the beneficial effect of WTD in term of time saving during production.



**Fig. 1.** The effect of WTD/kenaf fibre hybrid filler loading on cure time ( $t_{90}$ ) of NR compounds



**Fig. 2.** IR spectrum of WTD

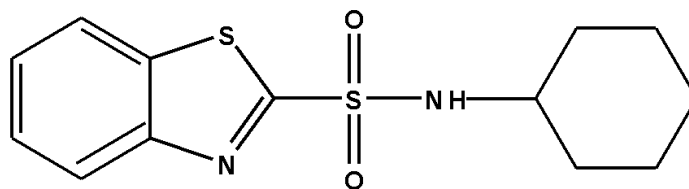


Fig. 3. The chemical structure of N-Cyclohexyl-2-benzothiazole sulfonamide (CBS)

### Scorch Time

Figure 4 shows the effect of WTD/kenaf fibre hybrid filler loading on the scorch time ( $t_2$ ) of NR compounds. From this figure, it can be seen that the value of  $t_2$  increases with the increment of kenaf fibre loading. Besides, this figure also exhibits an apparent increment of  $t_2$  with the addition of kenaf fibre. This could be due to the acidic effect from kenaf fibre. As reported by Neto et al. (2004) and Ohtani et al. (2001), uronic acid may exist in celluloses of kenaf fibre.

From IR spectrum of kenaf fibre shown in Fig. 5, the presence of  $-\text{COOH}-$  is demonstrated by a strong band at  $1728\text{ cm}^{-1}$  (Rashed et al. 2006). Furthermore, as reported by Ravichandran et al. (2004) and Arkema Inc. (2000), acidic materials incline to absorb the accelerator used for vulcanization, thus retarding the cure. Therefore the higher the loading of kenaf fibre, the longer the scorch time will be.

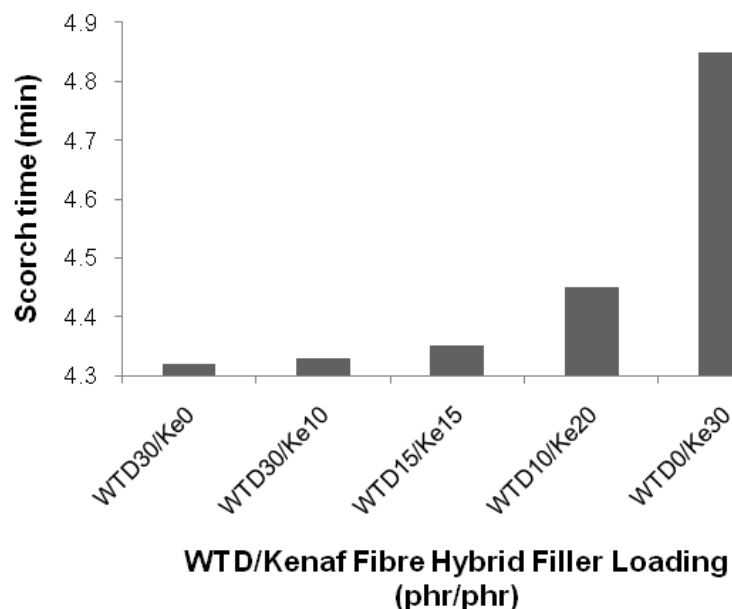


Fig. 4. The effect of WTD/kenaf fibre hybrid filler loading on the scorch time ( $t_2$ ) of NR compounds

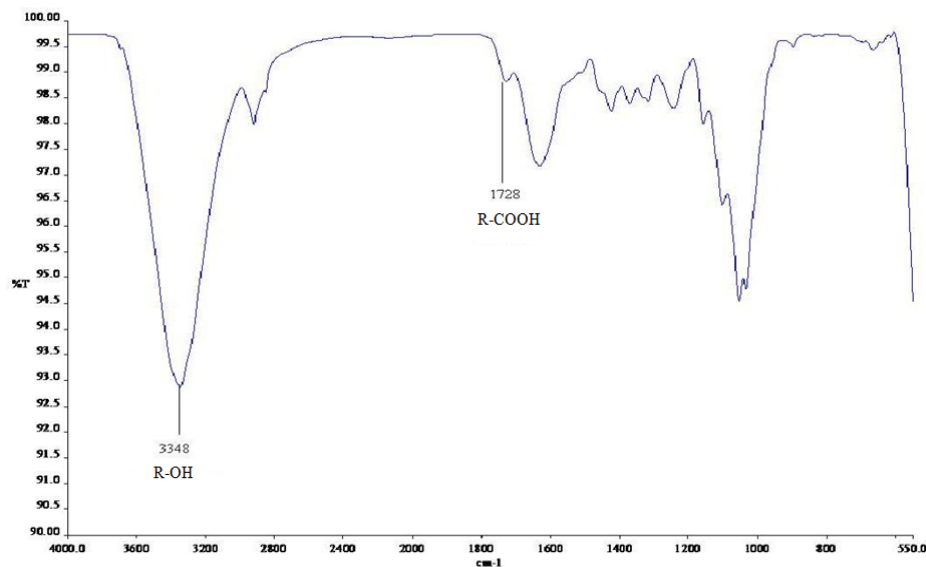


Fig. 5. IR spectrum of kenaf fibre

### Maximum Torque

Figure 6 shows the effect of WTD/kenaf fibre hybrid filler loading on maximum torque ( $M_{HR}$ ) of natural rubber compounds. From this figure it can be seen that the value of  $M_{HR}$  increased with the increment of kenaf fibre loading. As more kenaf fibre was added into NR compounds, the mobility of the macromolecular chains of NR also decreased, and this leads to increased value of  $M_{HR}$  (De et al. 2004). Therefore the higher kenaf fibre added into NR compound, the higher will be the rigidity and maximum torque.

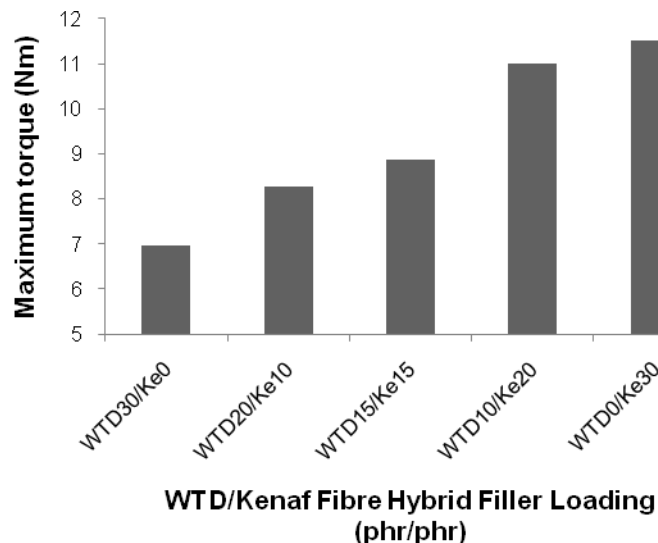


Fig. 6. The effect of WTD/kenaf fibre hybrid filler loading on maximum torque ( $M_{HR}$ ) of natural rubber compounds

## Tensile Strength

Figure 7 shows the effect of WTD/kenaf fibre hybrid filler loading on tensile strength of NR compounds. From this figure, it can be seen that there was a reduction in tensile strength of NR compounds with the addition of kenaf fibre. The reason behind this phenomenon is a lack of interfacial adhesion between kenaf fibre and NR matrix compared to the adhesion between WTD and NR.

As reported by Rashed et al. (2006), the presence of polar groups from hydroxyl and other polar group in natural fibre contributes to the incompatibility between natural fibre and non-polar matrix. The presence of hydroxyl group is shown in Fig. 5 and proven by the strong band at  $3348\text{ cm}^{-1}$  (Bruce 2007). Since natural rubber is a non-polar elastomer, it is incompatible with an essentially polar kenaf fibre, and this leads to decreasing value of tensile strength.

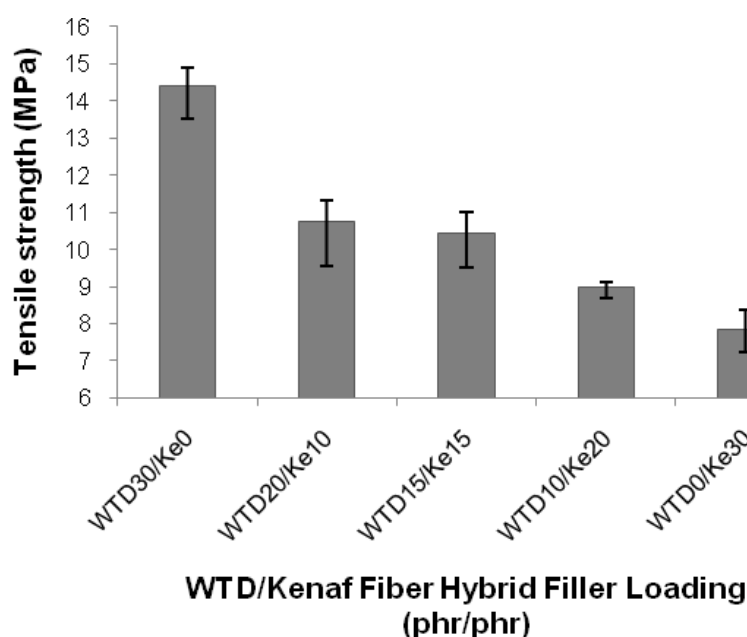


Fig. 7. The effect of WTD/kenaf fibre hybrid filler loading on tensile strength of NR compounds

## Elongation at Break

Figure 8 shows the effect of WTD/kenaf fibre hybrid filler loading on elongation at break of NR compounds. From this figure, it can be seen that there is apparent decrease of elongation at break with the addition of kenaf fibre. This is because of the stiffness effect from kenaf fibre. Kenaf fiber is a stiff fibre due to the presence of lignin (Bel-Berger et al. 1999).

Lignin, like celluloses, hemicelluloses, and ash (Mazuki et al. 2011) is a natural admixture found in kenaf. Consequently, the higher addition of kenaf fibre will stiffen and decrease the toughness of NR compound. Thus the higher the loading of kenaf fibre, the lower the value of elongation at break will be.



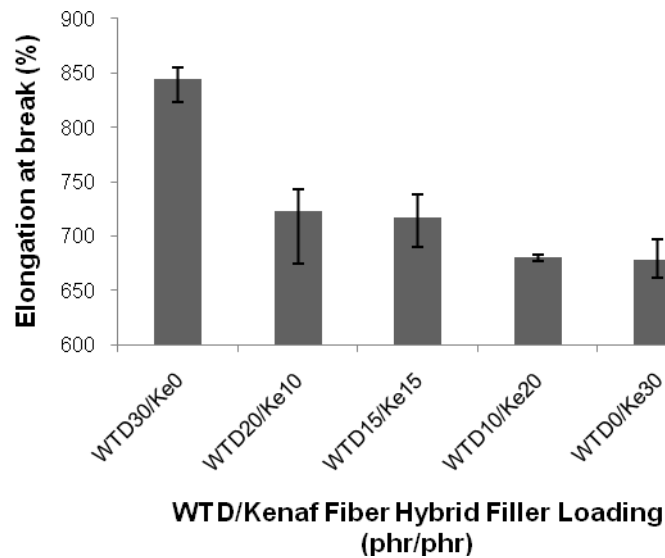


**Fig. 8.** The effect of WTD/kenaf fibre hybrid filler loading on elongation at break of NR compounds

### Stress at 100% and 300% Elongation

Figure 9 shows the effect of WTD/kenaf fibre hybrid filler loading on stress at 100% elongation ( $M100$ ) and stress at 300% elongation ( $M300$ ) of NR compounds respectively. From this figure, it can be seen that the value of  $M100$  and  $M300$  increased with the increment of kenaf fibre loading. This is due to the increment of stiffness with the addition of kenaf fibre. The increment of the value of  $M100$  and  $M300$  matched the results obtained from maximum torque. This strengthens the finding that the addition of kenaf fibre increases the stiffness of NR compounds. However, there was a decrease of  $M100$  and  $M300$  after the addition of 30 phr of kenaf fibre. This could be due to the agglomeration of kenaf fibre, as shown in the SEM morphological study.

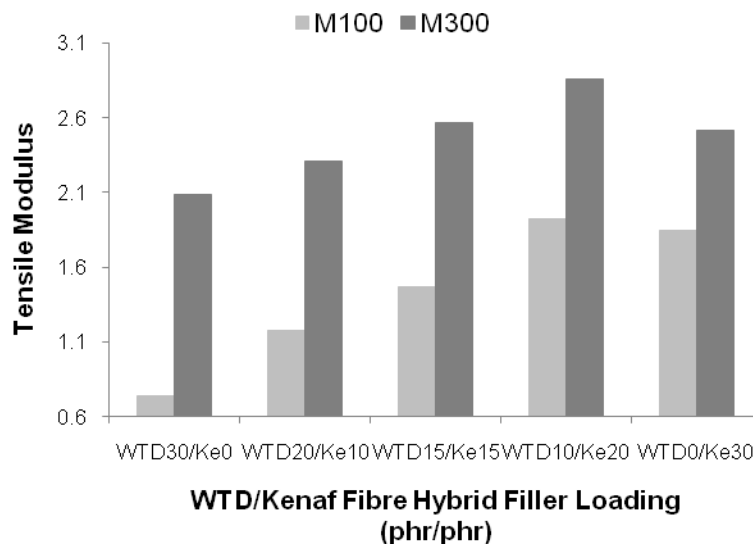


**Fig. 9.** The effect of WTD/kenaf fibre hybrid filler loading on stress at 300% elongation ( $M300$ ) of NR compounds

### Stress-Strain Behaviour

Figure 10 (a) exhibits the stress-strain curve of WTD/kenaf fibre hybrid filler filled NR compounds. This figure shows the highest and the lowest value of curve obtained by NR compound filled with merely 30 phr of WTD and 30 phr of kenaf fibre respectively.

At the first stage of drawing, it can be seen that more stress were applied to the NR compounds filled with 30 and 20 phr of kenaf fibre loading followed by the NR compounds filled with lower kenaf fibre loading. This figure also exhibits stiffer behaviour of NR compound filled with 20 phr of kenaf fibre loading as the highest amount of stress were applied on that compound from the initial to the failure stage. This proves the stiffness behaviour of kenaf fibre and also matches the result of tensile modulus. Nevertheless, the NR compound filled with 30 phr of kenaf fibre loading was the first to break and followed consequently by other NR compounds filled with lower kenaf fibre loading as shown in Fig. 10 (b). This shows that the NR compound filled with the highest kenaf fibre loading had the most brittle behaviour compared to the other NR compounds filled with lower kenaf fibre loading. Thus, these curves prove the results for tensile strength.

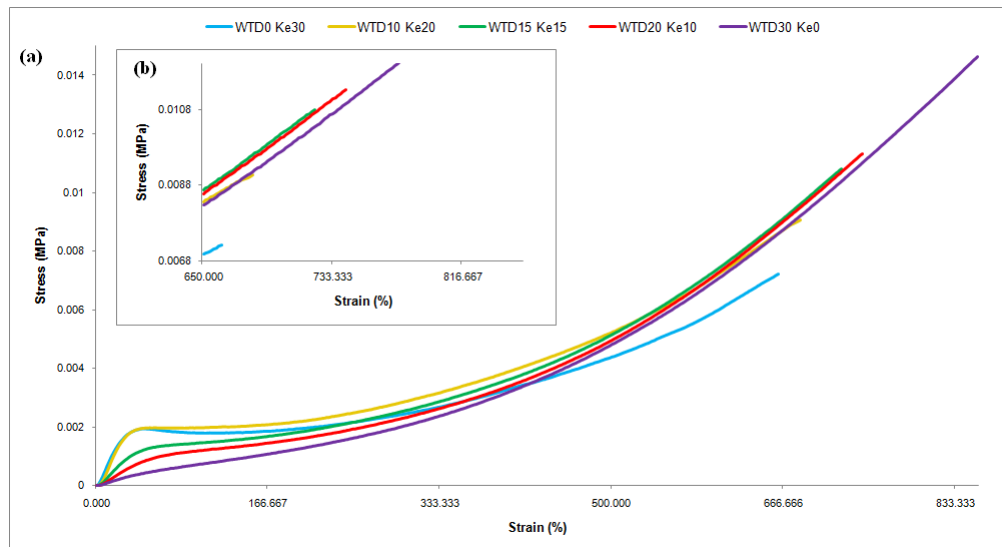


**Fig. 10.** (a) Stress-strain curve of WTD/kenaf fibre hybrid filler filled NR compounds, (b) Magnification of failure points of WTD/kenaf fibre hybrid filler filled NR compounds (inset)

### Fatigue Life

Figure 11 shows the effect of WTD/kenaf fibre hybrid filler loading on fatigue life of NR compounds. Based on this figure, the fatigue life decreased significantly after the addition of 10 phr of kenaf fibre. This again was due to the poor interfacial adhesion between kenaf fibre and NR matrix. From this figure, it can be seen that the interfacial adhesion between NR matrix and kenaf fibre was worse compared to the adhesion between WTD and NR matrix.

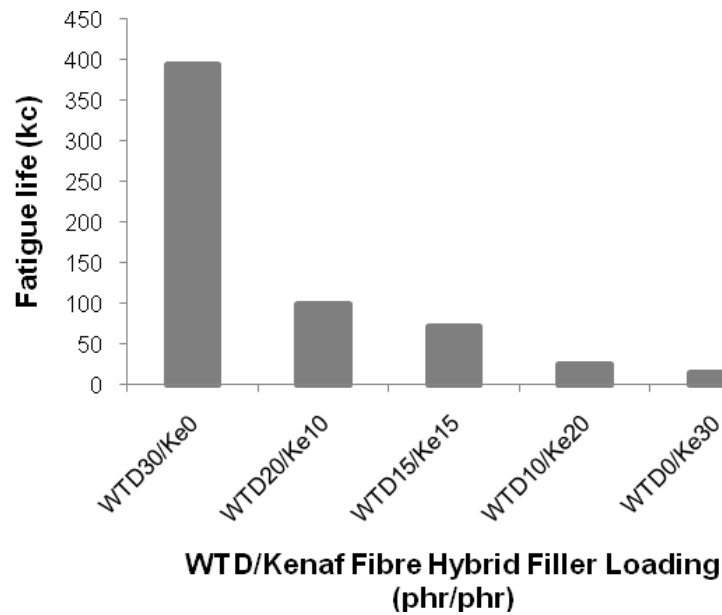


Fig. 11. The effect of WTD/kenaf fibre hybrid filler loading on fatigue life of NR compounds

### Rubber-Filler Interaction

Figure 12 shows the effect of WTD/kenaf fibre hybrid filler loading on rubber–filler interaction of NR compounds. Figure 12 shows that the value of  $Q_f/Q_g$  increased with the increment of kenaf fibre loading. Again, this result shows that the interfacial adhesion between NR matrix and kenaf fibre was poorer than WTD.

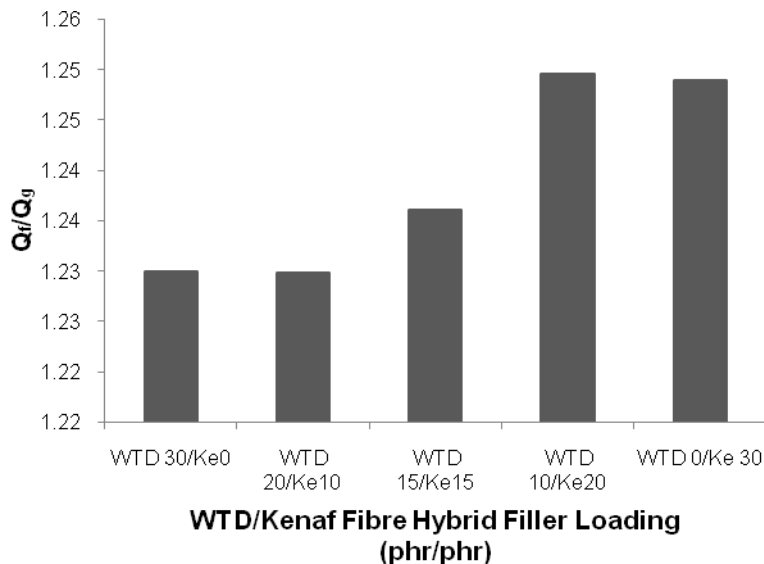
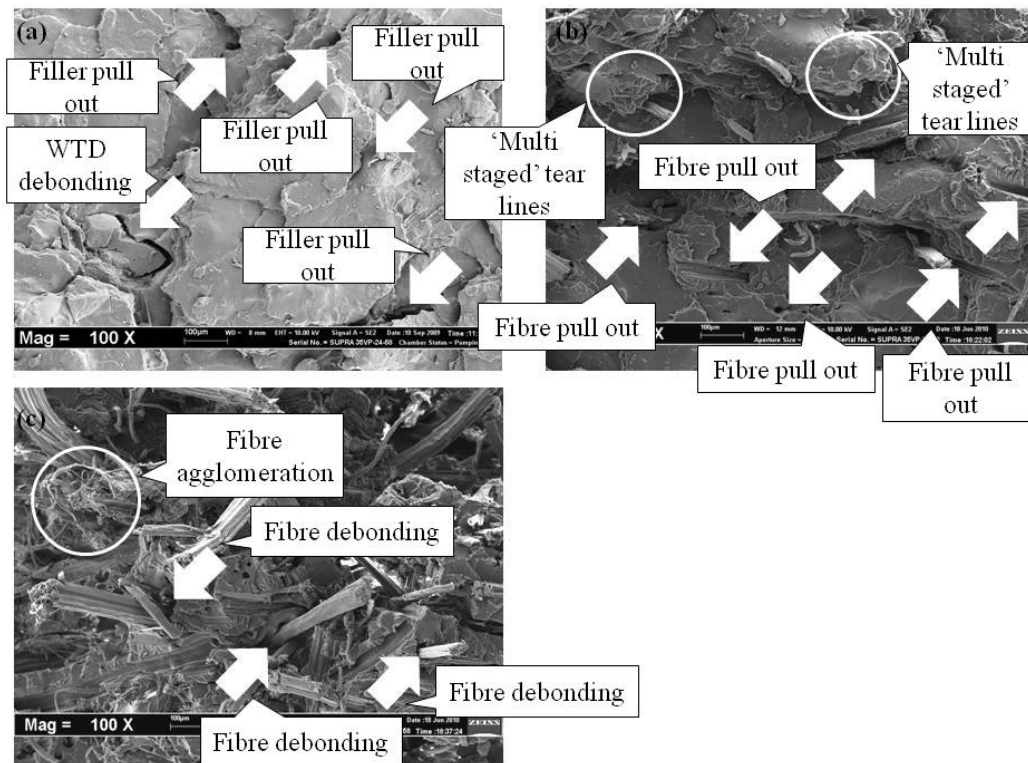


Fig. 12. The effect of WTD/kenaf fibre hybrid filler loading on rubber–filler interaction of NR compounds

### Morphological Study

Figure 13(a), 13(b), and 13(c) shows the tensile fractured surface for WTD/kenaf fiber hybrid filler filled NR compounds with 0 phr, 10 phr, and 30 phr of kenaf fibre respectively. Figure 13(a) shows tensile fractured surface of NR compound filled with 30 phr of WTD. From this figure it can be seen that there are traces of filler pull out and debonding of WTD particles from NR matrix (shown by arrow) due to lack of interfacial adhesion between NR matrix and WTD particles. In Fig. 13(b), there are also traces of fibre pull out (shown by arrows) due to the lack of interfacial adhesion. However, there are more tear lines on the tensile fractured surface in Fig. 13(b) compared to the one in Fig. 13(a). In addition, the fractured surface is coarser than in Fig. 13(a), and the tear lines also deeper and more ‘multi-staged’ (shown in circles). This is due to the increment of stiffness after the addition of 10 phr of kenaf fibre, as there is more force needed to break the sample. Besides, this also strengthens the result of *M100* and *M300* from tensile modulus, which increased after the addition of 10 phr of kenaf fibre.



**Fig. 13.** SEM micrograph of tensile fractured surface of WTD/Kenaf fibre hybrid filler filled NR compounds: (a) 30WTD/0kenaf, (b) 20WTD/10kenaf, (c) 0WTD/30 kenaf (Magnification 100x)

As for Fig. 13(c), the fractured surface was rougher and there were more fibres pulled out than in Fig. 13(b). Besides, fibre debonding (shown by arrow) and trace of fibre agglomeration (shown in circle) can also be seen in this figure. This is due to higher stiffness effect and also less interfacial adhesion between NR matrix and kenaf fibre after the addition of 30 phr of kenaf fibre. This matches the lowest value obtained in tensile strength for NR compound filled with 30 phr of kenaf fibre. Besides, this also strengthens the decreasing value of *M100* and *M300* after the addition of kenaf fibre.

Figure 14(a), 14(b), and 14(c) show the fatigue fractured surface for WTD/kenaf fiber hybrid filler filled NR compounds with 0 phr, 10 phr, and 30 phr of kenaf fibre respectively. Based on Figure 14(a), many tear lines appear on the fractured surface, and there are also WTD particles embedded in NR matrix (shown by arrow). This shows a good interfacial adhesion occurred between WTD particles and NR matrix. Consequently, this signifies the highest value of fatigue life obtained by NR compound filled with 30 phr of WTD. On the other hand, Fig. 14(b) exhibits fewer tear lines on the fractured surface. In addition, fibre debonding and pull-out can also be seen in this figure (shown by arrow). This is due to lack of interfacial adhesion between kenaf fibre and NR matrix compared to the interfacial adhesion between NR matrix and WTD particles, as shown by the significant decrease of value of fatigue life after the addition of 10 phr of kenaf fibre.

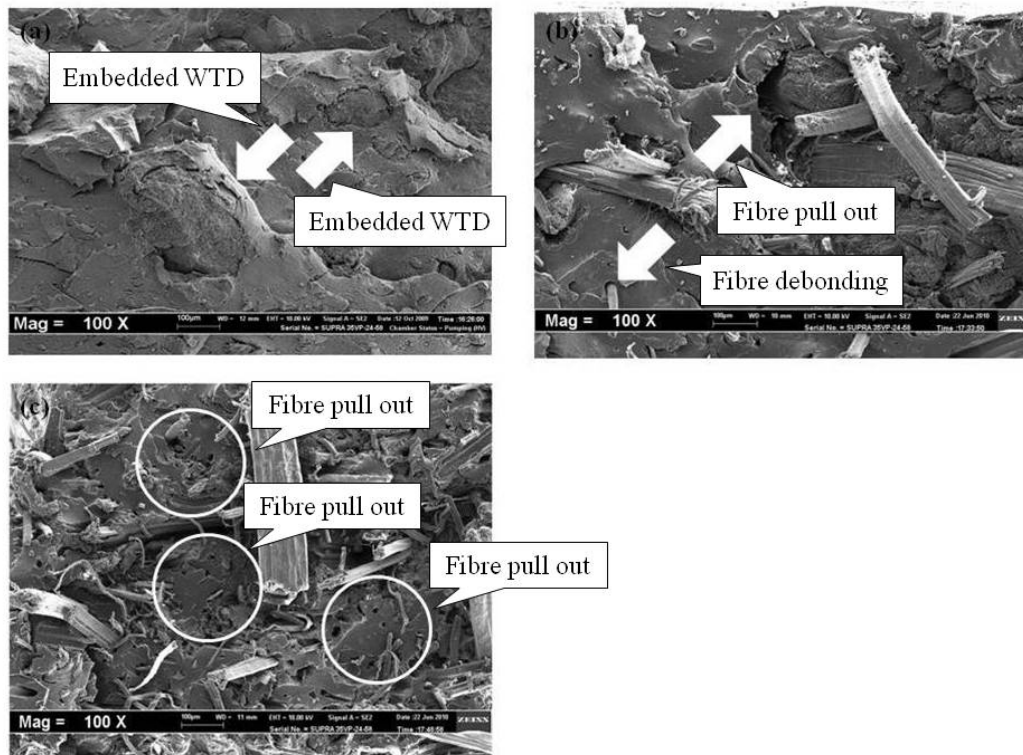


**Fig. 14.** SEM micrographs of fatigue fractured surface of WTD/kenaf fibre hybrid filler filled NR compounds: (a) 30WTD/0 kenaf, (b) 20WTD/10 kenaf, (c) 0WTD/30 kenaf (Magnification 100 $\times$ )

Figure 14(c) shows tear lines that were the lowest compared to that seen in Fig. 14(a) and 14(b). Besides, there were also more traces of fibre pull-outs in this figure compared to Fig. 14(b) (shown in circles). This is because as the fibre loading increases, the ability of NR matrix to wet kenaf fibre also decreases due to the low interfacial adhesion between NR matrix and kenaf fibre. Therefore, this verifies the lowest fatigue life value obtained for NR compound filled with merely 30 phr of kenaf fibre.

## CONCLUSIONS

1. The curing characteristics obtained show that the increment of partial replacement of WTD by kenaf fibre increases the value of cure time ( $t_{90}$ ), scorch time ( $t_2$ ), and maximum torque ( $M_{HR}$ ).
2. The increment of partial replacement of WTD by kenaf fibre decreases the value of tensile strength and elongation at break. The values of  $M100$  and  $M300$  increase with increasing kenaf fibre loading but decrease after the addition of merely 30 phr of kenaf fibre loading.
3. For fatigue life, the increment of partial replacement of WTD by kenaf fibre decreases the value of fatigue life of WTD/kenaf fibre hybrid filler filled NR compounds.
4. For rubber-filler interaction, the increment of partial replacement of WTD by kenaf fibre increases the value of rubber-filler interaction,  $Q_f/Q_g$ .
5. For SEM analysis, the increment of partial replacement of WTD by kenaf fibre decreases amount of tear lines and increases the coarseness and the amount of fibre pull outs from the tensile and fatigue fractured surface of WTD/kenaf fibre hybrid filler filled NR compounds.

## REFERENCES CITED

- Awang, M., and Ismail, H. (2009). "Weatherability of polypropylene/waste tire dust blends: Effects of trans-polyoctylene rubber and dynamic vulcanization," *Journal of Vinyl & Additive Technology* 15, 29-38.
- Bada, B. S., and Raji, K. A. (2010). "Phytoremediation potential of kenaf (*Hibiscus cannabinus* L.) grown in different soil textures and cadmium concentrations," *African Journal of Environmental Science and Technology* 4(5), 250-255.
- Bel-Berger, P., Hoven, T. V., Ramaswamy, G.N., Kimmel, L., and Boylston, E. (1999). "Cotton/kenaf fabrics: A viable natural fabric," *The Journal of Cotton Science* 3, 60-70.
- Benazzouk, A., D., O., Mezreb, K., Laidoudi, B., Quéneudec, M. (2008). "Thermal conductivity of cement composites containing rubber waste particles: Experimental study and modeling," *Construction and Building Materials* 22, 573-579.
- Bruice, P. Y. (2007) *Organic Chemistry*, 4<sup>th</sup> Edition, Pearson Education Inc, New Jersey.
- De, D., De, D., and Adhikari, B. (2004). "The effect of grass fiber filler on curing characteristics and mechanical properties of natural rubber," *Polymer for Advanced Technologies* 15, 708-715.
- ECHO® A (2009). "Cost-effective, high-performance vulcanizing agent for chlorinated Polyethylene," Arkema Inc. Technical Information, Philadelphia.
- Hamid, M. R. A. (2008), "Kenaf to replace tobacco: Farmers in Kedah to go for

- plants attributed to various items,” *Berita Harian’s* news update.
- Huda, M. S., Mohanty, A. K., Drzal, L. T., Misra, M., and Schut, E. (2004). “Physico-mechanical properties of “green” composites from poly (lactic acid) and cellulose fibres,” *Global Plastics Environmental Conference*, Detroit, USA.
- Lorenz, O., and Parks, C. R. (1961). “The crosslinking efficiency of some vulcanizing agents in natural rubber,” *Journal of Polymer Science* 50, 299-312.
- Mazuki, A. A. M., Akil, H. M., Safiee, S., Ishak, Z. A. M., and Bakar, A. A. (2011). “Degradation of dynamic mechanical properties of pultruded kenaf fibre reinforced composites after immersion in various solutions,” *Composites Part B: Engineering* 42(1), 71-76.
- Neto, C. P., Seca, A., Fradinho, D., Coimbra, M. A., Domingues, F., Evtuguin, D., Silvestre, A., and Cavaleiro, J. A. S. (1996). “Chemical composition and structural features of the macromolecular components of *Hibiscus cannabinus* grown in Portugal,” *Industrial Crops and Products* 5, 189-196.
- Ohtani, Y., Mazumder, B. B., and Sameshima, K. (2001). “Influence of the chemical composition of kenaf bast and core on the alkaline pulping response,” *Japan Wood Science* 47, 30-35.
- Park, J. K., Edil, T. B., Kim, J. Y., Huh, M., Lee, S. H., and Lee, J. J. (2003). “Suitability of shredded tyres as a substitute for a landfill leachate collection medium,” *Waste Management Resources* 21, 278-289.
- Rashed, H. M. M. A., Islam, M. A., and Rizvi, F. B. (2006). “Effects of process parameters on tensile strength of jute fiber reinforced thermoplastic,” *Journal of Naval Architecture and Marine Engineering* 3, 1-6.
- Ravichandran, K., and Natchimuthu, N. (2005). “Vulcanization characteristics and mechanical properties of natural rubber–scrap rubber compositions filled with leather particles,” *Polymer International* 54, 553-559.
- Segre, N., P. J. M. M. and Sposito, G. (2002). "Surface characterization of recycled tire rubber to be used in cement paste matrix," *Journal of Colloid and Interface Science* 248, 521-523.
- Stuart, B. H. (2004). *Infrared Spectroscopy: Fundamentals and Applications*, John Wiley & Sons Ltd., West Sussex.
- Suzuki, K., Kimpara, I., and Funami, K. (2004). “Finite element modeling of fine structure of natural plant fibres for statistical characterization of their tensile strengths,” *Composites Technologies for 2020: Proceedings of the Fourth Asian-Australasian Conference on Composite Materials (ACCM-4)*. Sydney, Australia.
- Tampere University of Technology, (2011). *Sulfur vulcanization*. [online] Available at: <[http://www.tut.fi/plastics/vert/5\\_rubber\\_chemistry/2\\_sulfur\\_vulcanization.htm](http://www.tut.fi/plastics/vert/5_rubber_chemistry/2_sulfur_vulcanization.htm)> [Accessed 15 July 2011].
- Yilmaz, A., and N. D. (2009). "Possibility of using waste tire rubber and fly ash with Portland cement as construction materials," *Waste Management Resource* 29, 1541-1546.

Article submitted: May 6, 2011; Peer review completed: June 26, 2011; Revised version received and accepted: August 3, 2011; Published: August 5, 2011.